KSCE Journal of Civil Engineering (2021) 25(8):3054-3063
DOI 10.1007/s12205-021-1880-1

pISSN 1226-7988, eISSN 1976-3808
www.springer.com/12205

Structural Engineering

Life Prediction Model of Nano-$CaCO_3$ Modified Concrete in Sulfate Environment

Theogene Hakuzweyezu[a], **Hongxia Qiao**[a,b], **Chenggong Lu**[a], **Bo Yang**[a], **and Kan Li**[a]

[a]*Western Engineering Research Center of Disaster Mitigation in Civil Engineering of Ministry of Education, Lanzhou University of Technology, Lanzhou 730050, China*
[b]*School of Civil Engineering, Lanzhou University of Technology, Lanzhou 730050, China*

ARTICLE HISTORY

Received 25 October 2020
Revised 15 February 2021
Accepted 15 March 2021
Published Online 12 May 2021

KEYWORDS

Concrete
Nano-$CaCO_3$
Sulfate corrosion
Wiener stochastic process
Life prediction
Reliability assessment

ABSTRACT

In the saline soil environment, the salts corrode the ordinary cement concrete seriously, and concrete structures deteriorate gradually until it fails, which impedes the practical application of ordinary Portland cement concrete in this area. Aiming at the durability problems of concrete in a harsh environment, this paper selects the coefficient of compressive strength, coefficient of flexural strength, relative dynamic elastic modulus, and relative mass to jointly evaluate the resistance of nano-$CaCO_3$ modified concrete to sulfate corrosion. More importantly, the Wiener process for modeling the degradation process of concrete specimens was used to obtain the remaining life's reliability function. The results indicated that adding 1% nano-$CaCO_3$ (Nano Calcium Carbonate) can enhance the resistance of concrete to sulfate corrosion, and the service life of concrete will increase significantly. The Random Wiener process can effectively predict the durability deterioration process of concrete specimens. By integrating the deterioration process's life data, this method's reliability function may directly reflect the concrete's life.

1. Introduction

Concrete has been widely used as a structural material for constructing coastal structures and tall buildings under harsh environments. Modern concrete materials must have high strength, toughness, and durability in order to meet the requirements of these applications (Jawad et al., 2020; Maheswaran et al., 2021). The topic related to sustainability and the durability of cementitious structures has attracted the scientific researcher and is still in a chaotic state. Actually, the concrete durability manifests the comprehensive effect of its material properties and the external service environment, which significantly influences the service life of concrete structures (Adil et al., 2020). In the actual service environment, especially the saline soil environment in western China under the combined effects of climate and environment, the concrete has deteriorated due to the presence of corrosive ions mainly SO_4^{2-}, Mg^{2+}, Cl^-, CO_3^{2-}, and the service life of concrete structures often fails prematurely before reaching the design life (Man et al., 2016; Huang et al., 2019). Unfortunately, this brings severe losses to the global economy and brings serious safety hazards to human production and life. Therefore, improve the durability of concrete structures and exploring new corrosion-resistant modified concrete materials is of great engineering significance.

Recently, nanomaterials have received widespread attention, and researchers have begun to incorporate them into concrete as admixtures (Du et al., 2019). As one of the most important construction materials in the 21st century, nanomaterials will undoubtedly bring about tremendous changes to building materials and even construction engineering. In response to the deterioration of concrete durability. Scholars have found that nanomaterials enhance concrete's mechanical properties and increase its durability (Kumar and Yuvaraj, 2020). Based on the economic and practicality, this research chooses relatively low-priced nano-$CaCO_3$ as the concrete admixture to study the durability of nano-modified concrete. Recent studies have shown that nano-$CaCO_3$ has varying mechanical properties than ordinary nano-$CaCO_3$ (Uthaman et al., 2019; Zhao et al., 2020). Regarding the sulfate corrosion resistance of nano-$CaCO_3$ modified concrete, Zhang Maohua and Li Xuecheng mixed 1%, 2%, and 3% nano-$CaCO_3$ into

CORRESPONDENCE Hongxia Qiao qhxlut7706@163.com Western Engineering Research Center of Disaster Mitigation in Civil Engineering of Ministry of Education, Lanzhou University of Technology, Lanzhou 730050, China; School of Civil Engineering, Lanzhou University of Technology, Lanzhou 730050, China

ordinary concrete. They found that with the addition of nano-$CaCO_3$, the sulfate corrosion resistance of nano-modified concrete improved, and when the nano-$CaCO_3$ content was 2%, the sulfate corrosion resistance was the best (Maohua and Xuecheng, 2018). Owing to its advantages in their properties through physical effects and low price, nano $CaCO_3$ is extensively used in cementitious composites. Research has shown that incorporating nano-$CaCO_3$ in concrete as admixtures is not detrimental to their mechanical properties (Mao et al., 2018; Maheswaran et al., 2021). However, the agglomeration phenomenon of nano $CaCO_3$ will greatly decrease its effectiveness (Hakamy, 2020; Mahadevaswamy and Suresha, 2020). The research on nano-$CaCO_3$ demonstrated that Nano-$CaCO_3$ mainly exerts its filling effect, chemical activity, nucleation effect, and other functions in concrete (Assaedi, 2020; Tian and Gao, 2020). It can optimize the structure of the interface transition zone to improve the durability and strength of concrete materials (Niu et al., 2020). The surface electron structure and crystal structure of nano calcium carbonate particles are altered due to their ultra-fineness, resulting in remarkable effects including quantum effect, size effect, surface effect, and interface effect, which are not observed in ordinary calcium carbonate (Cosentino et al., 2020; Yang, 2020; Zhao et al., 2020). The nano calcium carbonate calcite crystal's surface structure is close to that of C-S-H, so it has apparent hydration acceleration effects for cementitious materials. Han examined the influence of nano-fiber content on the anti-chloride ion permeability; the study founded that with the increasing nano-content, its penetration performance on the concrete is improved (Han et al., 2012). Sato and Diallo investigated the impact of nano-$CaCO_3$ on cement hydration, and the study found that the rapid growth of C-S-H was greatly enhanced by the addition of nano-$CaCO_3$ due to its seeding effect (Sun et al., 2020). Thus, nanomaterials with outstanding properties can enhance the mechanical properties, durability, and sustainability of cementitious materials. In an effort to evaluate the reliability of structures, reliability life prediction methods help the early detection and maintenance of the structure to ensure the long-term safe operation and durability of engineering structures (Wang et al., 2019; Li et al., 2020). Among the various existing life distributions, Wiener stochastic process as a probabilistic method has been widely used to realize the evaluation and prediction life of concrete in a corrosive environment (Hong et al., 2020). Moreover, based on fundamental mathematical models, Hongxia set up an indoor concrete life test in the simulated environment, and selected concrete 'dynamic elastic modulus as failure threshold; based on three-parameter Weibull distribution demonstrated reliability function and predicted residual life of concrete from the experimental data (Guo et al., 2019). Qiao simulated the saline soil area using wet sand containing compound salt solution as an electrolyte; the reliability function based on Wiener distribution was demonstrated by taking the measured corrosion current density as the failure threshold and predicting reinforced concrete's remaining life (Qiao et al., 2016). Based on the damage mechanics principle, Wang established the concrete damage parabola model to predict recycled concrete life after the freeze-thaw cycle (Wang et al., 2011). Thus, predicting the service life of concrete is crucial for improving the reliability, service life, and safety of the concrete structure and carrying out post-reinforcement maintenance. In the present work, aiming at the short service life of concrete in saline soil area, different evaluation indexes and test schemes have been chosen to assess nano-$CaCO_3$ modified concrete's performance exposed to sulfate attack. The performance degradation indicators were selected based on the measured life data to study nano-$CaCO_3$ modified concrete's remaining life under the sulfate environment, hoping to provide a high-performance concrete for engineering construction.

2. Experimental Details

2.1 Raw Materials

A Sinoma Gansu Cement Company produced the cement used in this study, its Chemical Composition and performance index are shown in Tables 1 and 2. Coarse aggregate with a mud content of 0.60% (by mass) and an apparent density of 2,650 kg/m^3 was used. Fine aggregate came from the river in a local area with a mud content of 2.1% (by mass), an apparent density of 2,600 kg/m^3, and a fineness modulus of 2.9. Other experimental materials included Class II fly ash produced by Lanzhou No.2 thermal power plant. The general tap water that meets the requirements of “Water Standard for Concrete Mixing” (JGJ63-2006, 2018) was used. The water-reducing agent used in the test was a high-performance polycarboxylic acid produced by Gansu Jifa Chemical Co., Ltd with a water-reducing rate of 25% and a mixing amount of 2.2%. The performance indicators of nano-$CaCO_3$ used in the experiment are shown below in Table 3.

Table 1. Chemical Composition of P·O 42.5 Ordinary Portland Cement

Ingredients	Ignition loss	SiO_2	Al_2O_3	Fe_2O_3	CaO	MgO	SO_3	Alkali content
Measured value (%)	1.92	24.08	8.54	4.01	58.29	1.73	2.85	0.5

Table 2. Performance Index of P·O 42.5 Ordinary Portland Cement

Stability	Specific surface area (m^2/kg)	Condensation time (min)		Flexural strength (MPa)		Compressive strength (MPa)	
		Initial setting	Final setting	3d	28d	3d	28d
Qualified	338	176	280	5.3	7.3	18.3	45.7

Table 3. Performance Indicators of Nano-$CaCO_3$

Appearance	Average particle size (nm)	Quality score /%	Specific surface area (m^2/g)
White powder	≤ 60	≥ 99.0	30

Table 4. Performance Indexes of Fly Ash

Moisture content/%	Water demand/ml	Fineness /%	Activity index /%
3.6	2.63	2.9	2,600

2.2 Mix Proportions

The design of concrete mix was based on "Common Concrete Mix Ratio Design Specification" (JGJ55-2011, 2011), "Common Concrete Mixture Performance Test Method" (GB/T 50080-2002, 2002), and "Concrete Strength Inspection and Evaluation Standard" (GB/T 50107-2010, 2010) and other specifications, the matching ratio for each specimen is shown below in Table 5.

2.3 Methods

In this test, a series of six concrete specimens were all cast in steel molds. The size of specimens was 100 mm × 100 mm × 400 mm; specimens were named as A0, A1, A2, A3, A4 and A5 with respect to mass fraction of Nano-$CaCO_3$ of 0%, 1%, 2%, 3%, 4%, and 5%. The soaking solution used in this test was 10% Na_2SO_4 solution. After 28 days of curing, the concrete samples were fully immersed in the solution. The test duration was 360d and the test solution was replaced every 30 days to ensure the accuracy of the test results and the freshness of the solution. Before collecting data, wipe the specimen's surface to prevent the surface solution from affecting the test results, and collect data every 60 days. The HC-U83 multi-functional concrete ultrasonic detector tested the ultrasonic sound velocity of the specimen, the quality of the sample was tested by the electronic balance with an accuracy of 0.1 g, the electric flexural testing machine tests the flexural strength of the specimen and the compressive strength of the specimens was tested by a microcomputer-controlled pressure testing machine.

2.4 Mechanical Test Activity

During the service period, the concrete is deteriorated by harmful ions and other factors, the performance gradually declines, and appearance changes. Therefore, this test's durability evaluation index was the coefficient of compressive strength, the coefficient of flexural strength, relative dynamic elastic modulus, and the relative mass to evaluate the nano-modified concrete's performance sulfate resistance jointly.

2.4.1 Calculation of Coefficient of Compressive Strength and Coefficient of Flexural Strength

Combining with the requirements corrosion resistance coefficient of concrete in "Test Method for Long-term Performance and Durability of Ordinary Concrete" (GB/T50082-2009, 2009), the calculation of K_α in this test is as follows:

$$K_\alpha = \frac{R_2}{R_1}, \tag{1}$$

where R_1 refers to the average measured value of the compressive strength of concrete specimens (MPa) after the concrete has been corroded in the solution for a certain number of days. R_2 refers to the average measured value of compressive strength of concrete specimens after soaking in clear water for a certain number of days (MPa); when $K_\alpha < 0.8$, the concrete reaches failure. The formula for calculating the coefficient of flexural strength K_β in this test is as follows:

$$K_\beta = \frac{R_2}{R_1}. \tag{2}$$

2.4.2 Calculation of Relative Mass W_r

Relative mass calculation formula: (Qiao, 2007)

$$W_r = \frac{W_n}{W_0} \times 100, \tag{3}$$

where W_r is the relative mass (%) of the material at different erosion ages; W_n is the mass value of the material (kg) when the erosion age is n days; W_0 is the initial mass value of the material (kg).

2.4.3 Calculation of Relative Dynamic Elastic Modulus

The relative dynamic elastic modulus was calculated as below:

$$E_r = \frac{E_t}{E_0} = \frac{V_t^2}{V_0^2}. \tag{4}$$

From the formula: E_t is the dynamic elastic modulus of the concrete when the erosion age is t days; E_0 is the initial dynamic

Table 5. Mix Proportions of Concrete

Specimen	Cement (kg/m^3)	Fly ash (kg/m^3)	Nano-$CaCO_3$ (kg/m^3)	Coarse aggregate (kg/m^3)	Fine aggregate (kg/m^3)	Water (kg/m^3)	Water reducing agent (kg/m^3)
A0	375	45	0	1,177	662	151	3.34
A1	370.8	45	4.2	1,177	662	151	3.34
A2	366.6	45	8.4	1,177	662	151	3.34
A3	362.4	45	12.6	1,177	662	151	3.34
A4	358.2	45	16.8	1,177	662	151	3.34
A5	354	45	21	1,177	662	151	3.34

elastic modulus of concrete. V_t is the ultrasonic sound velocity at a specific cycle time t, V_0 is the initial ultrasonic sound velocity of the concrete specimen.

3. Results and Discussion

Figure 1. illustrates the variation of corrosion resistance coefficient K_α (for compressive strength) of different specimens. With 180d as the critical age, the coefficient of compressive strength K_α of the specimens shows an upward trend from 0d to 180d (Fig. 1), indicating that as the immersion time increases, chemical reactions occur inside the concrete and as the internal compactness increases. Thus, the K_α value of concrete increases accordingly. The main reason is that the solution gradually enters into the concrete and the external pores and micro-cracks of the concrete, which generate corrosion products to fill the concrete's internal defects and increase the density of concrete. It can be seen that the increases of specimen A1 is the largest compared to other specimens with a rise of 11%, and the increase of A5 is the smallest compared with other specimens with only 9%.

Between 180d and 360d, the coefficient of compressive strength K_α of all specimens showed a downward trend, which indicates that the continuous entry of the sulfate solution inside the concrete caused excessive corrosion products to be generated inside the concrete. The internal concrete density reduces, and the K_α value decreases accordingly. At 360d, the K_α value of A1 decreased the least, only 7%, and the K_α value of A5 decreased the most, 14%. This is due to the internal stress caused by interior corrosion products gradually destroying the concrete's internal structure. At 360d, the K_α values of the specimens from large to small are A1 > A2 > A0 > A3 > A4 > A5, indicating that when the nano-$CaCO_3$ content is 1%, the effect of improving the sulfate resistance of concrete is the best.

Figure 2. illustrates the variation of corrosion resistance coefficient for flexural strength. It is clear that the increase of A1 is the largest among other test specimens with a rise of 17%, and the increase of A5 is the smallest compared to other specimens with an increase of 8%. At 360d, the K_β value of A1 decreased the least, only 7%, and the K_β value of A4 decreased the most, 17%. At 360d, the K_β value of the specimen from large to small is A1 > A3 > A2 > A0 > A5 > A4, indicating that when the nano-$CaCO_3$ content is 1%, the internal compactness of the sample is the best. Combining Figs. 1 and 2, the coefficient of flexural strength K_β of concrete is more sensitive than the coefficient of compressive strength K_α. There are two main stages in the change of corrosion resistance coefficient of the concrete. The first stage is the rising stage; as the immersion time increases, the solution gradually enters the interior of the concrete from the pores on the surface of the concrete and chemically reacts with the concrete hydration products to form corrosion products that fill the internal pores and micro-cracks of the concrete, and the concrete density increases. There is a rapid decline in the second stage; as Na_2SO_4 enters the concrete's interior, the corrosion products generated continue to increase, and the expansion stress caused by the corrosion products inside the concrete gradually increases compactness of the concrete decreases accordingly; K_α value and K_β value decrease accordingly. Based on the deterioration law of K_α and K_β value, when the nano-content is 1%, the test

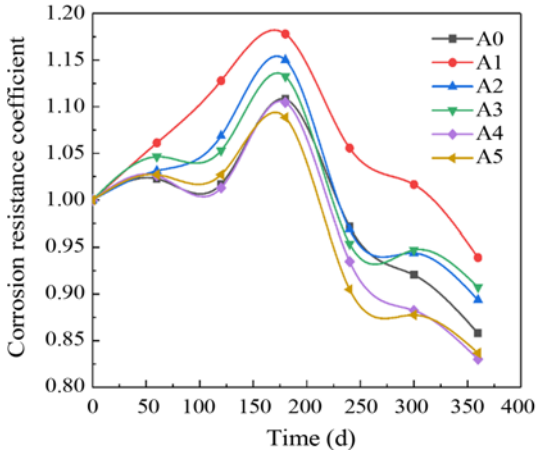

Fig. 2. The Rate Curves of Corrosion Resistance Coefficient K_β (for flexural strength) of Different Specimens

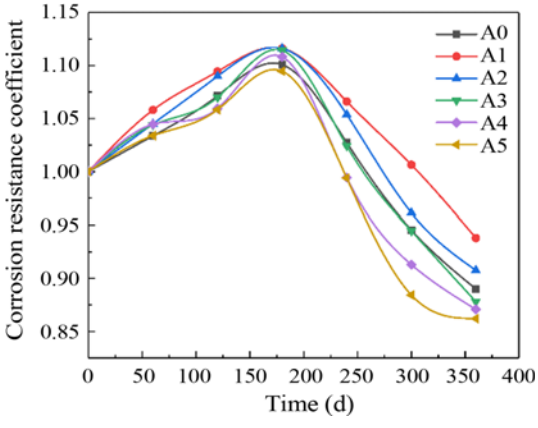

Fig. 1. The Rate Curves of Corrosion Resistance Coefficient K_α (for compressive strength) of Different Specimens

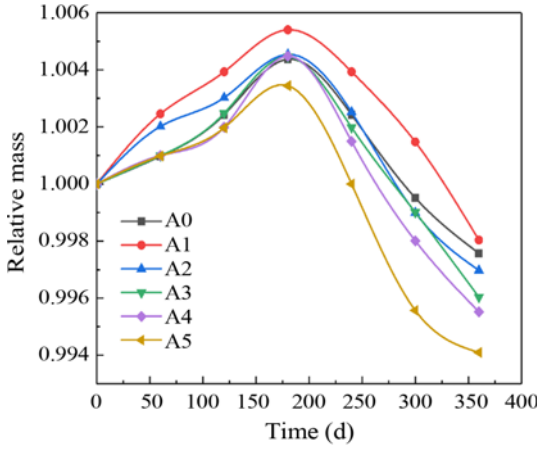

Fig. 3. The Rate Curves of the Relative Mass of Concrete Specimens at Different Immersion Ages

specimen has the best sulfate corrosion resistance. Fig. 3 shows the changes in the relative mass of concrete specimens at different immersion ages. The relative mass W_r of the specimens shows an upward trend from 0 to 180d, mainly due to the SO_4^{2-} enter inside the concrete to generate corrosion products, which increases the quality of the concrete and as well as the value of W_r.

The mass increase of the A1 specimen is the largest among the test specimens with an increase of 0.005%, and the increase of A5 is the smallest with an increase of 0.003%. Between 180d and 360d interval, the cementitious material inside the concrete was gradually dissolved out, and the value of W_r decreased accordingly. At 360d, the W_r value of A1 decreased the least, only 0.2%, and the W_r value of A5 decreased the most, with 0.6%. At 36d, the W_r value of the specimen is as follows: A1 > A0 > A2 > A3 > A4 > A5. Fig. 4 describes the rate changes of relative dynamic elastic modulus of concrete specimens different nano-$CaCO_3$. The relative dynamic elastic modulus is the non-destructive method used to evaluate concrete performance under sulfate corrosion from the aspect of the internal compaction of concrete (Desire et al., 2019; Niu et al., 2020). When the curing time increased, they were a moderate increase in concrete elasticity in the early ages. It is clearly shown that the E_r value of A5 increases slightly at 180d, with an increase of 20.2%, while A0 increases the least, increasing by 12.1%.

Between 180d and 360d, the E_r of all the specimens showed a downward trend. As the immersion age increases, the number of internal corrosion products in the concrete gradually increases, and the internal expansion stress also gradually increases. As a result, the internal compactness of concrete decreases, and the value of concrete E_r decreases accordingly. At 360d, the E_r value of A1 has the smallest drop, which is only 13.9%, and the E_r value of A5 has the most significant decrease, which is 26.0%. At 360d, the E_r value of the samples in descending order is A1 > A0 > A2 > A3 > A4 > A5, indicating that when the nano-content is 1%, the corrosion resistance of the sample is the best. It is noteworthy that the addition of nano-$CaCO_3$ can improve the elastic modulus of concrete. When nano-$CaCO_3$ reacts with tricalcium aluminate, the specific reaction process is as follows:

$$3CaO\cdot Al_2O_3 + Ca(OH)_2 + 12H_2O \rightarrow 4CaO\cdot Al_2O_3\cdot 13H_2O \quad (5)$$

Due to cement contains part of gypsum, the following reactions occur:

$$4CaO\cdot Al_2O_3\cdot 13H_2O + 3CaSO_4\cdot 2H_2O + 17H_2O \rightarrow 3CaO\cdot Al_2O_3\cdot 3CaSO_4\cdot 31H_2O + Ca(OH)_2, \quad (6)$$

$$3CaCO_3 + 4CaO\cdot Al_2O_3\cdot 13H_2O + 19H_2O \rightarrow 3CaO\cdot Al_2O_3\cdot 3CaCO_3\cdot 31H_2O + Ca(OH)_2, \quad (7)$$

$$3CaO\cdot Al_2O_3\cdot 3CaCO_3\cdot 31H_2O + 2(4CaO\cdot Al_2O_3\cdot 13H_2O) \rightarrow 3(3CaO\cdot Al_2O_3\cdot CaCO_3\cdot 12H_2O) + 2Ca(OH)_2 + 19H_2O. \quad (8)$$

Combining Eqs. (5), (6) and (8), we get

$$CaCO_3 + 12H_2O + 3CaO\cdot Al_2O_3 \rightarrow 3CaO\cdot Al_2O_3\cdot CaCO_3\cdot 12H_2O, \quad (9)$$

$$CaCO_3 + 12H_2O + 3CaO\cdot Al_2O_3 \rightarrow 3CaO\cdot Al_2O_3\cdot CaCO_3\cdot 12H_2O. \quad (10)$$

It can be seen from Eqs. (9) and (10) that during the hydration process, nano-$CaCO_3$ reacts with tricalcium aluminate to form hydrated calcium aluminate, which is more stable than ettringite. Moreover, this reaction can also reduce the content of tricalcium aluminate, reduce the amount of calcium aluminate hydrated when the specimen is attacked by sulfate, thereby improving the corrosion resistance of concrete. When the specimen is cured for 28 days and immersed in a sulfate solution, the following reactions will occur:

$$Na_2SO_4\cdot 10H_2O + Ca(OH)_2 \rightarrow CaSO_4\cdot 2H_2O + 2NaOH + 8H_2O, \quad (11)$$

$$3(CaSO_4\cdot 2H_2O) + 4CaO\cdot Al_2O_3\cdot 12H_2O + 14H_2O \rightarrow 3CaO\cdot Al_2O_3\cdot 3CaSO_4\cdot 31H_2O + Ca(OH)_2. \quad (12)$$

From Eqs. (11) and (12), it can be seen that the cement hydration product will react with sulfate solution to form ettringite, and ettringite is less soluble, its chemical structure combines a lot of crystal water, and the volume is about 2.5 times that of calcium aluminate hydrate. The mineral form is also needle-like crystals, which form hedgehog-like formations on the surface of calcium aluminate hydrate solid phase, causing greater internal stress inside the concrete. With the increase of erosion age, the durability evaluation index showed a trend of rising first and then falling, and the specimens gradually destroyed. The formation of dihydrate gypsum, whose volume is twice that of calcium hydroxide, will cause concrete damage due to excessive internal expansion stress.

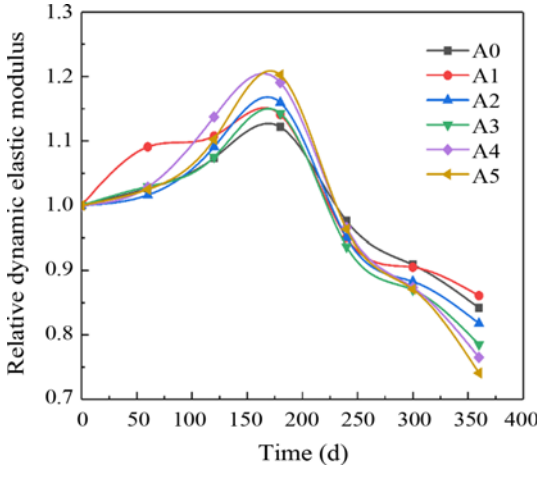

Fig. 4. The Rate Curves of the Relative Dynamic Elastic Modulus of Concrete Specimens at Different Immersion Ages

4. Modeling Based on Wiener Stochastic Process

Recently, because of its ability to capture the random variance of failure times due to various patterns or levels of cyclic forces,

statistical models are typically used for the failure times of fatigue failure data. The random Wiener process is a type of Brownian Motion with linear drift parameters. In 1923, Wiener described "irregular motion" as a random process and explained it through mathematics (Yin et al., 2015). It is among the most widely used random process in probability theory worthy of describing the non-monotonic degradation of product performance with increasing or decreasing trends caused by various damage factors (Kui et al., 2018). The Wiener stochastic process modeling has stable, easy calculation and analysis (Wang et al., 2014). Thus, considering the engineering applicability, Wiener stochastic process can be directly used to evaluate concrete reliability under different degradation indicators.

4.1 Model Description

The experimental results are utilized as statistical input parameters in a probabilistic deterioration model. This experiment assumes that the univariate Wiener degradation process can demonstrate the degradation process of concrete durability. The actual value of the concrete performance degradation measured at time t is $D(t)$, and the observed value is recorded as $Z(t)$. Due to the measurement error in the actual observation process, therefore

$$Z(t) = D(t) + \varepsilon \ . \tag{13}$$

Among them, ε is the measurement error, which is not considered in this experiment, then

$$Z(t) = D(t) \ . \tag{14}$$

Since the durability degradation trend of concrete is a random process, Brownian motion can be described with offset; the durability deterioration process of concrete by the Wiener random process is

$$D(t) = f(t) + \sigma W(t) \ . \tag{15}$$

Among them, $D(t)$ is the degradation amount of concrete at time t, $f(t)$ is the deterministic polynomial trend, σ is the diffusion coefficient in the degradation stage, and $W(t)$ is the standard Brownian motion, $E[W(t)] = 0$, $E[W(t_1)W(t_2)] = min(t_1, t_2)$. In the process of concrete durability degradation, if the degradation amount $D(t)$ of its performance parameters at time t satisfies the following properties, the durability deterioration process can be simulated by the Wiener process:

1. $\Delta D(t)$ is the increment of degradation from time t to $t+\Delta t$, and $\Delta D(t)$ meets the requirements of the normal distribution, namely $\Delta D(t) \sim N(\mu\Delta t, \sigma 2\Delta t)$.
2. In any two non-intersection intervals $[t1, t2]$ and $[t3, t4]$ ($t1 < t2 \le t3 < t4$), the increment of the degradation amount $D(t1) \sim D(t2)$ and $D(t3) \sim D(t4)$ are independent of each other.
3. At $t = 0$, $D(0) = 0$, and the amount of degradation is continuous.

To meet the above properties, the Wiener process can establish a model of concrete durability degradation. When performing reliability analysis based on performance degradation data, it is necessary to establish a degradation model describing product performance degradation. It is also essential to determine the failure threshold of product failure. The failure threshold of the durability evaluation index of the specimen is related to the termination criterion of durability life, and it is the boundary value for judging whether the product is in a "normal" state (Yan et al., 2020). The selection of the failure threshold of the specified durability evaluation index was based on the "Test Method for Long-term Performance and Durability Performance of Ordinary Concrete" (GB/T 50082-2009, 2009). According to the relevant regulations in GB/T 50082-2009, it is stipulated that when the mass loss reaches 5%, or the dynamic elastic modulus loss reaches 40%, the concrete specimen reaches the failure state. Assuming that the concrete specimen's failure threshold is Df, selecting the failure threshold of the specified durability evaluation index of the test specimen is shown in Table 6.

Table 6. Failure Threshold of Each Durability Evaluation Index

Evaluation index	Failure threshold D_f
Coefficient of compressive strength K_α	0.2
Coefficient of flexural strength K_β	0.2
Relative mass W_r	0.05
Relative dynamic elastic modulus E_r	0.4

When the K_α, K_β, W_r, and E_r loss of the test specimen reach 0.2, 0.2, 0.05, and 0.4, the test piece is considered invalid. When the evaluation index of the test specimen first degrades to the failure threshold Df, the time is

$$T = \inf\left\{t \middle| D(t) \ge D_f, t \ge 0\right\}. \tag{16}$$

From Eq. (8), the remaining life distribution function of concrete is as follows:

$$F(t) = p(T \le t) = p(D(t) \ge D_f) = p(W(t) \ge \frac{D_f - \mu t}{\sigma}) = \Phi(\frac{\mu t - D_f}{\sigma\sqrt{t}}) + e^{2\mu D_f/\sigma^2}\Phi(\frac{-\mu t - D_f}{\sigma\sqrt{t}}) \ , \tag{17}$$

where $F(t)$ is the inverse Gaussian distribution of T;

$p(W(t) \ge \frac{D_f - \mu t}{\sigma})$ is the probability of $W(t) \ge \frac{D_f - \mu t}{\sigma}$;

$\Phi(\frac{\mu t - D_f}{\sigma\sqrt{t}})$ is the distribution function of the standard normal distribution with $\frac{\mu t - D_f}{\sigma\sqrt{t}}$ parameter;

$\Phi(\frac{-\mu t - D_f}{\sigma\sqrt{t}})$ is the distribution function of the standard normal distribution $\frac{-\mu t - D_f}{\sigma\sqrt{t}}$.

The probability density function of the residual life of concrete is as follows:

$$f(t) = \frac{D_f}{\sqrt{2\pi\sigma^2 t^3}} e^{-\frac{(D_f - \mu t)^2}{2\sigma^2 t}} \ . \tag{18}$$

Due to the nature of the normal distribution, for any time t, its

expectation and variance are

$$E(T)=\frac{D_f}{\mu}, \tag{19}$$

$$Var(T)=\frac{D_f\sigma^2}{\mu^3}. \tag{20}$$

The reliability function is as follows:

$$R(t)=1-F(t)=\Phi(\frac{D_f-\hat{\mu}t}{\hat{\sigma}\sqrt{t}})-e^{\frac{2\hat{\mu}D_f}{\hat{\sigma}^2}}\Phi(\frac{-D_f-\hat{\mu}t}{\hat{\sigma}\sqrt{t}}), \tag{21}$$

$\Phi(.)$ is the standard normal distribution function.

4.2 Parameter Estimation

A total of m specimens of concrete were tested for sulfate resistance. For test piece i, the performance degradation amount at the initial time, t_0 is $D_{i0} = 0$, and the performance degradation amount of the test specimen is measured at time $t_1 \ldots t_{ni}$, and the measured value is

$$D=\begin{pmatrix} D(t_{11}) & \cdots & D(t_{1m}) \\ \vdots & \ddots & \vdots \\ D(t_{n1}) & \cdots & D(t_{nm}) \end{pmatrix}. \tag{22}$$

Let $\Delta x_{ij} = D_{ij} - D_{i(j-1)}$ be the performance degradation amount of test specimen i between time t_{j-1} and t_j, and its value is obtained as follows:

$$\Delta x_{ij}=\begin{pmatrix} \Delta x_{11} & \cdots & \Delta x_{1j} \\ \vdots & \ddots & \vdots \\ \Delta x_{i1} & \cdots & \Delta x_{ij} \end{pmatrix}. \tag{23}$$

According to the nature of the random wiener distribution, we know

$$\Delta x_{ij} \sim N(\mu\Delta t_j, \sigma^2\Delta t_j), \tag{24}$$

where $\Delta t_j = t_j - t_{(j-1)}$; $i = 1, \ldots\ldots, m$; $j = 1, \ldots\ldots, n$. The likelihood function obtained from the performance degradation data is

$$L(\mu,\sigma^2)=\prod_{i=1}^{m}\prod_{j=1}^{n_i}\frac{1}{\sqrt{2\sigma^2\pi\Delta t_j}}\exp\left[-\frac{(\Delta x_{ij}-\mu\Delta t_j)}{2\sigma^2\Delta t_j}\right]. \tag{25}$$

From Eq. (17), the maximum likelihood estimation of the parameters μ and σ^2 required by Wiener can be obtained as

$$\hat{\mu}=\frac{\sum_{i=1}^{m}D_{in_i}}{\sum_{i=1}^{m}t_{ni}}, \hat{\sigma}^2=\frac{1}{\sum_{i=1}^{m}n_i}\left[\sum_{i=1}^{m}\sum_{j=1}^{n_i}\frac{(\Delta x_{ij})^2}{\Delta t_{ij}}-\frac{(\sum_{i=1}^{m}D_{in_i})^2}{\sum_{i=1}^{m}t_{n_i}}\right], \tag{26}$$

where $\hat{\mu}$ is the estimated value of the mean value of the overall life distribution; $\hat{\sigma}^2$ is the estimated value of the variance of the overall life distribution.

4.3 Reliability Assessment

Substitute Eqs. (22), (23) and (26) into K_α, K_β, E_r, and W_r obtained from the actual measurement and calculation of the specimen under full immersion to get the parameter estimation value, and then substitute the parameter estimation value into the Eq. (21) and calculate the reliability curve of the test specimen by Matlab R2014b. The estimated values of parameters for each specimen are given in Table 6. The durability of concrete specimens gradually deteriorates with time; when the reliability is below a reliability level that has been set, the specimen reaches in the failure state, and the durability of life is terminated. Based on the whole specimen's life data, the parameter estimation of the overall specimen was prevailed. According to the trajectory change of the evaluation indexes, the entire specimen's reliability function curve was obtained, which illustrates the Wiener stochastic process's effectiveness for the durability life prediction.

Figures 5 and 6 illustrate the individual reliability function curve of the relative mass W_r and Relative dynamic elastic modulus E_r for each specimen obtained. It can be seen from Fig. 5 that the reliability of relative mass W_r for specimen A1 at 1,500d is 0.068746, for the specimen A0 is 0.04624. From Fig. 6, the reliability of relative dynamic elastic modulus obtained for the A1 specimen at 1,500d is 0.174452, for specimen A5 is 0.03760, indicating that the addition of 1% nano-$CaCO_3$ can significantly

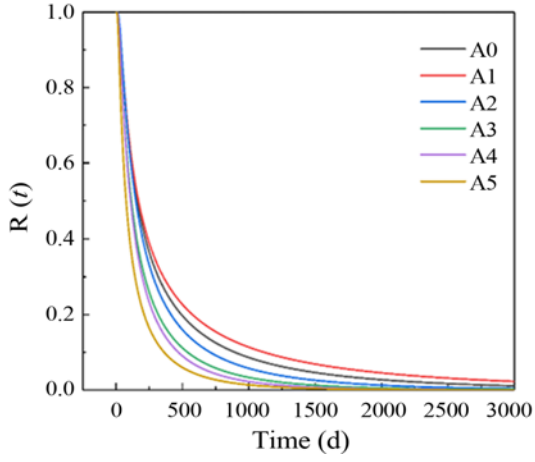

Fig. 5. Relative Mass W_r

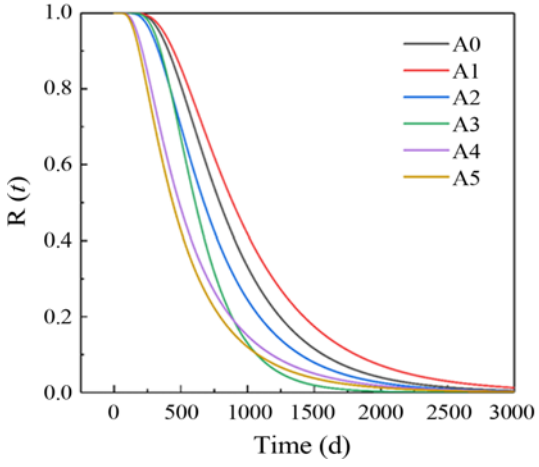

Fig. 6. Relative Dynamic Elastic Modulus E_r

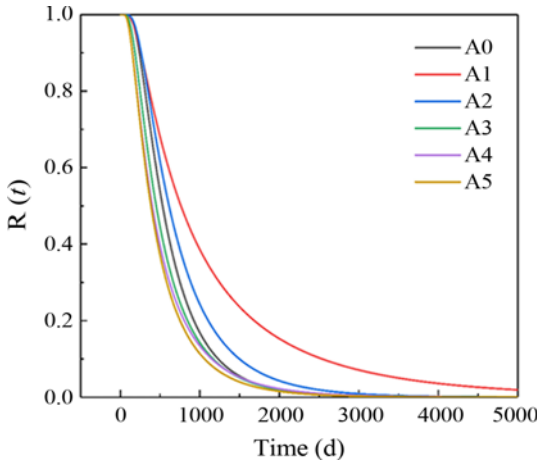

Fig. 7. Coefficient of Compressive Strength K_α

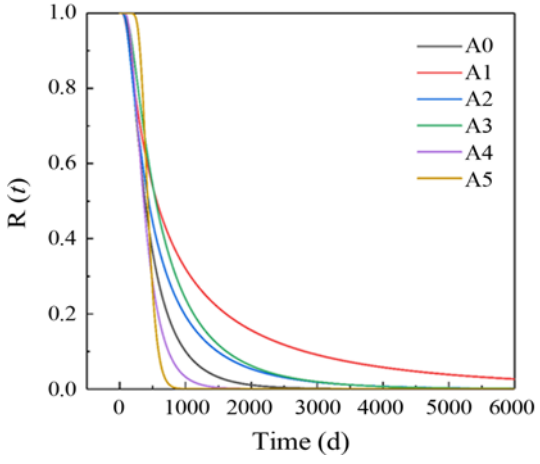

Fig. 8. Coefficient of Flexural Strength K_β

improve the sulfate resistance of concrete in the fully immersed state.

Based on the concrete competition failure criterion, the reliability obtained from the coefficient of compressive strength of the A1 specimen at 5,000d is 0.019164; for specimen A5, the value of K_α is 0.000102. The reliability obtained from the coefficient of flexural strength of specimen A1 at 5,000d is 0.038539. In addition, it can be seen from the prediction results that the remaining life of the fully immersed concrete specimens under the sulfate environment is also different with the different content of nano-$CaCO_3$. Among them, the remaining life of A1 is the longest, the remaining life of A5 is the shortest, and the remaining life in descending order is: A1 > A2 > A0 > A3 > A4 > A5. This proves that when the content of nano-$CaCO_3$ is 1%, the specimen has high reliability. Too much content will lead to a decrease in the concrete's sulfate resistance in the fully immersed state, which will reduce the service life of the concrete. Therefore, this can indicate that concrete durability prediction is effective using the Wiener process, which is in good agreement with the actual results and has high reliability. The directive significance is that the reliable level can be set higher when applying the Wiener stochastic process to assess the actual concrete structure's service life.

5. Conclusions

After the indoor full-immersion state, the resistance of nano-$CaCO_3$ modified concrete to the sulfate corrosion was analyzed based on various durability evaluation indicators. The durability evaluation indicators showed an upward trend during the early stage from 0 to 180d and a downward trend from 180 d to 360 d. Through this research, the main conclusions can be summarised below:

1. The appropriate incorporation of nano-$CaCO_3$ enhances the internal concrete structure. It increases the strength of concrete specimens, which dramatically improves the impermeability of concrete and prevents the intrusion of external harmful ions. However, the agglomeration phenomena of nano-$CaCO_3$ can reduce its effectiveness significantly.
2. Wiener stochastic process may well predict the deterioration process of concrete specimens for durability. By incorporating the life data of the deterioration process, the reliability function demonstrated in this method can reflect the concrete specimen's life. This method is easy in the calculation and has a certain value of application and popularisation. In engineering applications, the level of reliability may be adjusted to a higher degree so that the implementation of the relevant control measures can be carried out in advance.
3. The remaining life of concrete specimens under full immersion changes with the contents of nano-$CaCO_3$ added and the reliability curves of concrete specimens show a downward trend over time. Due to the different degradation indicators selected, the declining rate of the reliability curves is also different. When the content of nano-$CaCO_3$ is 1%, the sulfate resistance and life of the concrete structure are significantly increased.

Acknowledgments

The authors wish to acknowledge the financial support from China's National Natural Science Foundation No. 51168031 and 51868044.

ORCID

Theogene Hakuzweyezu https://orcid.org/0000-0002-4297-1273
Hongxia Qiao https://orcid.org/0000-0002-0289-1949
Chenggong Lu https://orcid.org/0000-0001-5394-664X

References

Adil G, Kevern JT, Mann D (2020) Influence of silica fume on mechanical and durability of pervious concrete. *Construction and Building Materials* 247:118453, DOI: 10.1016/j.conbuildmat.2020.118453
Assaedi H (2020) The role of nano-$CaCO_3$ in the mechanical performance

of polyvinyl alcohol fibre-reinforced geopolymer composites. *Composite Interfaces* 28(5):527-542, DOI: 10.1080/09276440.2020.1793096

Cosentino I, Liendo F, Arduino M, Restuccia L, Bensaid S, Deorsola F, Ferro GA (2020) Nano $CaCO_3$ particles in cement mortars towards developing a circular economy in the cement industry. *Procedia Structural Integrity* 26(2019):155-165, DOI: 10.1016/j.prostr.2020.06.019

Desire N, Qiao H, Li Y, Liang J (2019) The use of basalt rock powder and superfine sand as supplementary cementitious materials for friendly environmental cement mortar. *Research and Application of Materials Science* 1(1):1-9, DOI: 10.33142/msra.v1i1.665

Du S, Wu J, Alshareedah O, Shi X (2019) Nanotechnology in cement-based materials: A review of durability, modeling, and advanced characterization. *Nanomaterials* 9(9), DOI: 10.3390/nano9091213

GB 50080-2002 (2002) Standard for test method of performance on ordinary fresh concrete. GB/50080-2002, National Standard of the People's Republic of China, Beijing, China

GB/T 50082-2009 (2009) Standard for test methods of long-term performance and durability of ordinary concrete. GB/T 50082-2009, Ministry of Housing and Urban-Rural Development of the People's Republic of China, Beijing, China

GB/T 50107-2010 (2010) Standard for evaluation of concrete compressive strength. GB/T 50107-2010, Ministry of Housing and Urban-Rural Development of the People's Republic of China, Beijing, China

Guo X, Qiao H, Zhu B, Wang P, Wen S (2019) Accelerated life testing of concrete based on three-parameter weibull stochastic approach. *KSCE Journal of Civil Engineering* 23(4):1682-1690, DOI: 10.1007/s12205-019-0995-0

Hakamy A (2020) Effect of $CaCO_3$ nanoparticles on the microstructure and fracture toughness of ceramic nanocomposites. *Journal of Taibah University for Science* 14(1):1201-1207, DOI: 10.1080/16583655.2020.1809840

Han L, Danying G, Jun Z (2012) Research on the mechanical properties and anti-chloride ion permeability of fiber nano concrete. *Journal of North China Institute of Water Conservancy and Hydroelectric Power* 33(6):39-45

Hong F, Oiao H, Wang P (2020) Predicting the life of BNC-Coated reinforced concrete using the weibull distribution. *Emerging Materials Research* 9(2):1-10, DOI: 10.1680/jemmr.19.00087

Huang Q, Li Y, Chang C, Zheng W, Wen J, Dong J, Man Y, Danchun A, Xiao X, Zhou Y (2019) The compressive strength development of magnesium oxychloride cement comprising a composite additive in brine. *Ceramics - Silikaty* 63(4):347-355, DOI: 10.13168/cs.2019.0030

Jawad ZF, Salman AJ, Ghayyib RJ, Hawas MN (2020) Investigation the effect of different nano materials on the compressive strength of cement mortar. *AIP Conference Proceedings* 2213(1), DOI: 10.1063/5.0000164

JGJ55-2011 (2011) Specification for mix proportion design of ordinary concrete. JGJ55-2011, China Architecture & Building Press, Beijing, China

JGJ63-2006 (2018) Standard of water for concrete. JGJ63-2006, Ministry of Construction of the People's Republic of China, Beijing, China

Kui L, Yu D, Shaopo H, Al (2018) Prediction of residual electric life of AC contactor based on wiener process. *Proceedings of the Chinese Society of Electrical Engineering* 38(13):3978-3986+4039, DOI: 10.1080/21650373.2016.1218802

Kumar MM, Yuvaraj S (2020) Behaviour of different nanomaterials in geopolymer concrete. *International Journal of Innovative Technology and Exploring Engineering* 9(5):605-611, DOI: 10.35940/ijitee.e2462.039520

Li J, Qiao H, Zhu F (2020) Reliability analysis of fiber concrete freeze-thaw damage based on weibull method. *Emerging Materials Research* 9(1):1-9, DOI: 10.1680/jemmr.19.00110

Mahadevaswamy HS, Suresha B (2020) Role of nano-$CaCO_3$ on mechanical and thermal characteristics of pineapple fibre reinforced epoxy composites. *Materials Today: Proceedings* 22:572-579, DOI: 10.1016/j.matpr.2019.08.211

Maheswaran S, Ramachandra Murthy A, Ramesh Kumar V, Karunanithi A (2021) Characterisation studies on the particle size effect of calcium carbonate in high-strength concrete. *Magazine of Concrete Research* 1-13, DOI: 10.1680/jmacr.19.00375

Man D, Yin H, Cao M (2016) Research progress of concrete durability in saline soil environment. *Bulletin of the Chinese Ceramic Society* 35(11):3575-3580+3606, DOI: 10.16552/j.cnki.issn1001-1625.2016.11.013 (in Chinese)

Mao H, He B, Guo W, Hua L, Yang Q (2018) Effects of Nano-$CaCO_3$ content on the crystallization, mechanical properties, and cell structure of PP nanocomposites in microcellular injection molding. *Polymers* 10(10), DOI: 10.3390/polym10101160

Maohua Z, Xuecheng L (2018) Sulfate erosion resistance of nano-based concrete under freeze-thaw environment. *Journal of Natural Disasters* 27(02):94-99 (in Chinese)

Niu D, Zhang L, Fu Q, Wen B, Luo D (2020) Critical conditions and life prediction of reinforcement corrosion in coral aggregate concrete. *Construction and Building Materials* 238:117685, DOI: 10.1016/j.conbuildmat.2019.117685

Qiao H (2007) Evaluation method for durability of concrete against sulfate attack. PhD Thesis, College of Civil Engineering, Lanzhou University of Technology, Lanzhou, China (in Chinese)

Qiao H, Zhu B, Lu C, Feng Q, Zhou M, Cao H (2016) Accelerated life test of concrete based on wiener stochastic process. *Jianzhu Cailiao Xuebao/Journal of Building Materials* 19(6), DOI: 10.3969/j.issn.1007-9629.2016.06.012 (in Chinese)

Sun Y, Zhang P, Guo W, Bao J, Qu C (2020) Effect of Nano-$CaCO_3$ on the mechanical properties and durability of concrete incorporating fly ash. *Advances in Materials Science and Engineering* 2020, DOI: 10.1155/2020/7365862

Tian W, Gao F (2020) Effect of carbon nanotubes' diameter on freeze-thaw resistance of cement paste. *Journal of Mechanics* 36(4):437-449, DOI: 10.1017/jmech.2020.6

Uthaman S, George RP, Vishwakarma V, Harilal M, Philip J (2019) Enhanced seawater corrosion resistance of reinforcement in nanophase modified fly ash concrete. *Construction and Building Materials* 221:232-243, DOI: 10.1016/j.conbuildmat.2019.06.070

Wang PH, Qiao HX, Feng Q, Cao H (2019) Life prediction of coated steel with individual difference in magnesium oxychloride cement concrete. *Zhejiang Daxue Xuebao (Gongxue Ban)/Journal of Zhejiang University (Engineering Science)* 53(12):2309-2316, DOI: 10.3785/j.issn.1008-973X.2019.12.007 (in Chinese)

Wang H, Xu XT, Zhao JZ (2014) Residual life prediction method fusing accelerated degradation and field degradation data. *Hangkong Xuebao/Acta Aeronautica et Astronautica Sinica* 35(12):3350-3357 (in Chinese)

Wang LJ, Wang ZS, Cui ZL (2011) Life prediction of recycled concrete based on freeze-thaw damage parabolic model. *Journal of Applied Basic Science and Engineering* 19(1):29-35, DOI: 10.3969/j.issn.1005-0930.2011.01.004

Yan L, Wen Y, Teo KL, Liu J, Xu F (2020) Construction of regional logistics weighted network model and its robust optimization: Evidence from

China. *Complexity* 2020, DOI: 10.1155/2020/2109423

Yang J (2020) Effect of nano $CaCO_3$ on durability of concrete. *E3S Web of Conferences* 165:163-166, DOI: 10.1051/e3sconf/202016503029

Yin HL, Yang XH, Lu H (2015) A new bayesian method for reliability assessment of products with Wiener process degradation. *Journal of Tongji University* 43(8):1234-1238, DOI: 10.11908/j.issn.0253-374x.2015.08.017 (in Chinese)

Zhao Z, Qi T, Zhou W, Hui D, Xiao C, Qi J, Zheng Z, Zhao Z (2020) A review on the properties, reinforcing effects, and commercialization of nanomaterials for cement-based materials. *Nanotechnology Reviews* 9(1):349-368, DOI: 10.1515/ntrev-2020-0023